Characterisation of Waste Manganese Carbonate for Biooxidation Effluent Neutralisation*

[1]J. J. K. Gordon and [1]E. K. Asiam
[1]University of Mines and Technology, P.O. Box 237, Tarkwa, Ghana

Gordon, J. J. K. and Asiam, E. K. (2017), "Characterisation of Waste Manganese Carbonate for Biooxidation Effluent Neutralisation", *Ghana Journal of Technology,* Vol. 1, No. 2, pp. 51-61.

Abstract

The conventional chemical used in the neutralisation of biooxidation effluents is lime. The search for cheaper and readily available alternative reagents has been the motivation for a number of researches. This paper considered the characterisation and utilisation of Waste Manganese Carbonate (WMC) (waste-bearing manganese carbonate material) from Ghana Manganese Company in Ghana as a neutralising agent for biooxidation effluents. The WMC is composed of manganese carbonate (76.6%), dolomite (7.1%), muscovite (8.5%), quartz (6.5%), todorokite (0.3%) and the amorphous content was 1.0%. The elemental Mn content was approximately 28.26%. The Bond Index was 13.52 kWh/t, and the particle size distribution gave D_{50} as 5.89 µm. The isoelectric point (iep) of the WMC dispersed in MilliQ water occurred at ~pH 8.5, and the powder specific surface area measured was 6.12 m^2/g. WMC was used to neutralise biooxidation effluent with arsenic concentration of 1276 mg/L at pH 1.85 and 27 ^oC and it was able to deprotonate the effluent from pH 1.85 to 5.5 in 120 min depending on solid loading. Arsenic sequestration increased with increasing WMC concentration with residual arsenic concentration in solution ranging between 0.78 and 1.11 mg/L at pH 7.0. Surface area of the WMC precipitates was 12.62 m^2/g and the corresponding D_{50} values at pH 4.5 and 7.0 were respectively 5.89 µm and 10.35 µm. Mobile arsenic extracted from the precipitates averaged 4.135 mg/L at pH 7.0 and 1.594 mg/L at pH 7.4 as against the EPA maximum allowable concentration of 5.0 mg/L.

Keywords: Biooxidation Effluent Neutralisation, Waste Manganese Carbonate, Characterisation, Work Index.

1 Introduction

Currently, one major pretreatment process for complex auriferous flotation concentrates is bacterial oxidation (BIOX) using chemoli-thotrophic bacterial species for example *Acidithiobacilli* species (Lindström *et al*., 1992; Marshall *et al*., 1994; Bennet and Tributch, 1978; Olivier *et al*., 2000). The biooxidation process occurs in acidic medium and in pH ranges of 1.2 to 1.8 where sulphur and iron in the flotation concentrate are used up by microorganisms as energy sources to biotransform the concentrate. The valuable solid is prepared for gold extraction through cyanidtion. The effluent contains very high toxic ions which are environmentally dangerous base metals and require neutralisation before dumping in tailings embankments.

Calcium carbonate is currently used in treatment of bioeffluent in a two stage arsenic and heavy metals removal process of bioeffluent in place of lime (Pantuzzo and Ciminelli, 2010; Zhu *et al*., 2006; Swash and Monhemius, 2014; Swash and Monhemius, 1994; Du Plessis and Maree, 1994; Maree and Du Plessis, 1994; Hamester *et al*., 2012). Other researchers have also shown that, waste materials with calcium carbonate/oxide base have been tested on acidic effluents and they have proved to be suitable (Gahan *et al.,* 2010; Olivier, 2001). There are also some other carbonates in the rhombohedral carbonates group such as manganese carbonate (Wersin *et al*., 1989; Calvert and Price, 1972; Jensen *et al*., 2002). However this carbonate has not been investigated for neutralisation of biooxidation effluents.

Manganese carbonate is abundant in Ghana and has been exploited since the 1960s (Kesse,1985). In processing manganese carbonate ore for export, the material is crushed and screened and particle sizes below 25 mm are stockpiled as processing waste because the particle sizes are below client specification and are of no other commercial use. Generally, manganese carbonate dissolves in groundwater (K_{sp}= 2.24 x 10^{-11}) very slowly and is able to modify pH of ground water upwards. Manganese carbonate solubility in acid medium at ambient temperature has also been tested to raise pH beyond 5 (Duckworth and Martins, 2004).

Currently, two large biooxidation plants are operated by AngloGold Ashanti and Golden Star Resources among about eleven biooxidation plants in the world. These companies have blended alternatives to calcium hydroxide to achieve some success in processing the biooxidation effluent. Presently, no research work has been done anywhere to use the waste manganese carbonate as a substitute carbonate to process acidic biooxidation effluent. This study therefore aims at characterising waste manganese carbonate and to investigate its effect on neutralisation of biooxidation effluent.

*Manuscript received December 20, 2016
Revised version accepted March 16, 2017

2 Resources and Methods Used

2.1 Materials and Materials Preparation

Twenty litres (20 L) of biooxidation effluents obtained after counter-current decantation washing was obtained from the Sulphide Treatment Plant of AngloGold Ashanti, Obuasi. About 50 kg representative sample of WMC ore for the study was obtained from Ghana Manganese Company (GMC), Nsuta. Particle size distribution of the bulk material was conducted on the sample using the Tyler series method of sieve selection.

2.2 Bond Work Index Determination

About 10 kg dried WMC sample was used for Bond Ball Mill Work Index (BBMWI) determination. The standard Bond ball mill work index procedure was utilized (Napier-Munn, 1996). The procedure used for the test was repeated over a number of cycles till 250% circulating load was obtained. Equation 1 was used for the BBMWI calculation.

$$W_i = \frac{4.5}{P_{106}^{0.233} \times \left(G_{pb}\right)^{0.87} \times \left(\frac{1}{\sqrt{P_{80}}} - \frac{1}{\sqrt{F_{80}}}\right)} \quad (1)$$

where:
P_{106} is the size of test sieve used;
G_{pb} is the net grams undersize per revolutions;
P_{80} is the product 80% passing size in microns; and
F_{80} is the feed 80% passing size in microns.

The sample was crushed using a laboratory tertiary Jaw crusher to obtain 100% passing 4 mm sieve size. Part of this material was used for grindability studies and representative samples were split using the Jones riffle splitter, bagged and sealed for subsequent studies.

2.3 Pulverisation of Waste Manganese Carbonate

Labtenics LM 2 Laboratory Pulverizing Mill mounted on high compression spiral springs was used to mill the sample. The material was pulverized in batches using C-2000 (about 1 kg capacity) bowl with a disc (steel) as grinding medium and each sample was milled for 15 min. The mill was operated at a pressure of about 482.63 KNm^{-2}. The pulverized sample was used for subsequent studies.

2.4 Particle Size Distribution

The particle size of the powdered WMC sample was measured using Mastertersizer 2000 (Malvern Instruments Ltd, UK). The function of the instrument is based on the principle of static light scattering as monochromatic light which interacts with particles in water at room temperature. In the process, the particles diffract light proportional to their sizes. Thus, the diffraction patterns are then cumulatively processed to achieve the volume and mass size distribution of the particles.

2.5 Surface Area Determination

The specific surface area of WMC was measured by a 5-point N_2 adsorption BET method (Anon, 2015; Isa *et al*., 2014; Ticknor and Saluja, 1990; Brunauer *et al*., 1938) using Germini 2390 BET analyser (Micrometrics, USA). About 0.5 g representative sample was dried at 80 ºC for 24 hr in order to expel moisture and gases before measurements. The average value of the adsorption and desorption specific areas of the particles were considered as the real values.

2.6 Zeta Potential Determination

Interfacial chemistry of the WMC particles in KNO_3 (electrolyte) solution was determined by measuring the zeta potential (ζ) of the particles as a function of pH using Acoustosizer II Colloidal Dynamics equipment. The zeta potentials displayed good reproducibility within ±2.5 mV standard deviation at a confidence limit of about 0.1. The first zeta potential was calculated by fitting the theory to electroacoustics spectra with ESA size (or attenuation size if there is no ESA size). The second zeta potential was the Smolluchowski zeta which was also calculated from low frequency only using thin double layer static Smoluchowski formula which does not account for particle inertia or effects of concentration (Johnson *et al*., 2000).

2.7 Elemental and Mineralogical Investigations

The elemental compositions of the WMC were determined using X-ray Fluorescence (SECTROX-LAB-2000 XRF machine). In the process, about 4 g of WMC sample was weighed and about 0.9 g of non-reactive adhesive gum was then added and mixed thoroughly for about 3 min. The mixture was thereafter pressed into pellet using a 68.95 KNm^{-2} laboratory hydraulic pressure device. The pellet was then placed in the XRF analyser where the elements in the sample were measured.

The mineralogical composition was determined using Scintag ARL X'tradiffractometer CuKα radiation produced at 10 kV and 10 mA. Prior to measurement, approximately 10 wt% ZnO was added to the sample to ensure calculation of the

amorphous content of the sample. The X-ray diffraction traces were collected between 5°and 90° 2θ at 0.02° intervals at a rate of 0.05° per min. The mineral identification and quantification were conducted using XPowder and SIROQUANT V3 software. SEM analysis was also conducted using the Zeiss Evo Scanning Electron Microscope equipped with a Backscattered Electron (BSE) image detector.

2.8 Neutralisation of Bio-Effluent with WMC Powder

About 10 g/L, 20 g/L, 30 g/L, 40 g/L, 50 g/L and 60 g/L solid concentrations of WMC were added to the effluent for neutralisation at near room temperature (about 27 °C) using a 6-stirrer Lovibond Flocculator (Fig. 1) and stirred at 300 rpm. The pH and redox potentials of the slurries were monitored and measured at 30 min intervals for 300 min. The samples were filtered at the end of the period using 0.45 µm filter membrane. The filtrates were stored in clean labelled sample bottles for arsenic analysis.

Fig 1Six-stirrer Lovibond Flocculator

2.9 Stablity of WMC Precipitates Determination

Toxicity characteristic leach procedure (TCLP) is designed to determine the mobility of inorganic analytes present in solid precipitates. The precipitates obtained during the neutralisation stage were therefore leached to ascertain their stability in the environment.TCLP was thus carried out on the solid precipitates generated from the waste manganese carbonate neutralisation reactions. The TCLP calculation as developed by United States Environmental Agency (USEPA) is given in Equations 2 and 3.

$$[As]_{TCLP} = \frac{\text{Assay Value} \times \text{Mass of Preserved Extract}}{\text{Mass of TCLP Extract}} \quad (2)$$

and

$$\textit{Mobile As} = \frac{\text{Assay (Lab)Value} \times \text{Preserved Extract (wt)}}{\text{Mass of Sample}} \quad (3)$$

3 Results and Discussion

3.1 Particle size distribution of as received Sample

Particle size analysis conducted on the as-received waste manganese carbonate sample is shown in Fig. 2. It was observed that about 40 wt. % of the as-received material was retained on 4.75 mm screen which is an indication that the WMC was predominantly fine since the threshold particle size is 25 mm.

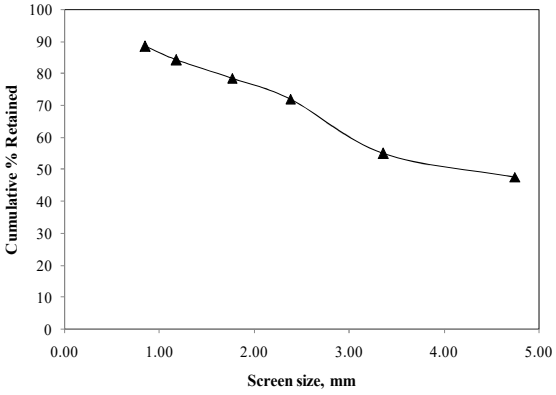

Fig. 2 Particle Size Distribution of As-received Waste Manganese Carbonate

3.2 Grindability Tests

The work index measured for the Waste Manganese Carbonate (WMC) sample was 13.5 kWh/t which compares with standard calcium carbonate sample (13.52 kWh/t) and therefore requires similar energy to efficiently mill the material. WMC is of medium hardness since its work index is between 9 and 14 kWh/t (Starkey and Meadows, 2007; Napier-Munn, 1996).

3.3 Particle Size Distribution (PSD) of Powdered WMC Sample

The particle size distribution analysis conducted on the powdered WMC using Laser diffraction (Malvern Mastersizer X, Malvern UK), gave the 10th, 50th and 90th percentiles denoted as 0.232 µm for D_{10}, 5.890 µm for D_{50} and 65.521 µm for D_{90} Furthermore, the specific surface area, pore volume and pore sizes measured using BET Analyser were 6.12 m^2/g, 0.012 cm^3/g and 8.41 nm respectively.

3.4 Zeta Potential of Powdered WMC Sample

The Zeta Potential measurement of the WMC sample used in this study is shown in Fig. 3. The particle Zeta Potential of WMC powder was negative at pH of 10 and increased to zero at pH of about 8.50, which is the isoelectric point (iep). The result correlates well with those obtained by Tsunekawa and Takamori (1987) who also showed that the iep value of pure $MnCO_3$ lies around pH 7.75. It can therefore be inferred that WMC has closely similar surface chemical properties. The difference in iep can be attributed to the purity of WMC. From pH 8.50, the zeta potential increased in the positive potential region and increased in magnitude from the alkaline region until ~ pH 5. The zeta potential then conscripted until pH 3. On the reverse sweep, the zeta potential increased in the opposite direction making the sweep incongruent. It then increased until ~ pH 4 when it became flat up to pH 5. The zeta potential then rose in magnitude as the pH sweep went from pH 5 to 7 from where it dropped from pH 7 to 9 into negative magnitude region and remained unchanged until pH 10. From Fig. 3, the iep extended beyond pH 7.75 and may be comparable to iep of $MnCO_3$ (iep of 7.75) as is indicated in Tsunekawa and Takamori (1987).

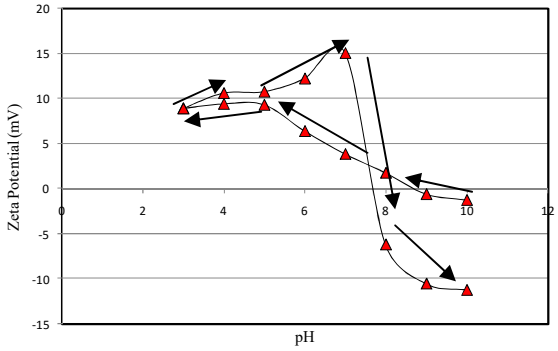

Fig. 3 Zeta Potential of 8 wt. % Solid WMC in 10^{-3} M KNO_3 as a Function of Solution pH. The Arrows Indicate the Direction of pH Sweep

3.4 Chemical and Mineralogical Composition of WMC

3.4.1 Elemental Analysis of WMC

The major elements identified in the WMC sample using X-ray Fluorescence (XRF) analysis are shown in Table 1 as Mn (28.26%) constituting the major element, Si (7.23%), Mg (3.31%), Ca (2.86%), Al (1.53%), Na (0.16%) and Fe (0.89%). It was observed that, Ca element content composed of less than 3% of the WMC sample.

Table 1 Major Elemental Composition

Elements	%	Elements	%
Na	0.16	S	0.2
Mg	3.31	Cl	0.0012
Al	1.53	K	0.16
Si	7.23	Ca	2.86
P	0.03	Mn	28.26
		Fe	0.89

The XRF analysis gave cobalt content of 1435 ppm and the rest of trace elements ranged from 4.4 to 603 ppm (Table 2). Each element identified has different impact on its applications. Thus, this elemental data could guide in the selection of WMC for any purpose.

Table 2 Trace Elemental Composition

Elements	ppm	Elements	ppm
Ti	603	As	152.1
V	227	Br	4.7
Cr	258	Rb	5.6
Co	1435	Sr	143
Ni	310.1	Zr	10.1
Cu	46.6	Mo	133.7
Zn	137.6	Cd	4.4
Ga	6.3	Sb	11.6
Ge	4.5	Ba	135.5

The major oxides detected by XRF analysis in the sample included 36.49% MnO, 15% SiO_2, 5.49% MgO and 4.01% CaO. The other oxides were below 3% as is shown in Table 3. Assessment of the oxide content is relevant as it gives information on the materials application for instance in acidic effluent treatment. About 0.5% SO_3 was measured as trace element as a major oxide.

Table 3 Major Oxides

Oxides	%	Oxides	%
Na_2O	<0.21	K_2O	0.197
MgO	5.49	CaO	4.01
Al_2O_3	2.904	TiO_2	0.101
SiO_2	15.47	MnO	36.49
P_2O_5	0.128	Fe_2O_3	1.267
SO_3	0.492	Cl	<0.0009

3.4.2 Mineralogical Composition of WMC

The mineralogical composition of WMC is shown in Table 4. The XRD results indicate 76.6% rhodochrosite as the major mineral present in the sample with muscovite (8.5%), dolomite (7.1%), quartz (6.5%) and todorokite (0.3%) as the minor minerals. An amorphous content of 1 % was also identified as unresolved minerals coupled with

about 10 wt. % of ZnO used to spike the sample. The carbonate content from the rhodochrosite is the prominent component in acid deprotonation processes.

Table 4 Mineral Composition of WMC

Minerals	Weight (%)
Rhodochrosite	76.6
Dolomite	7.1
Todorokite	0.3
Muscovite	8.5
Quartz	6.5
Amorphous	1.0

The morphology of the WMC particles in Fig. 4 showed plate-like shapes and mixture of large and fine size distribution of the particles at 10 µm scale. The particles surfaces were fairly smooth which is indicative of grinding of the material. X-ray spectra collected on some particles of the WMC sample have shown high presence of some elements which suggests presence of minerals and these points are labelled A to G in Fig. 4.The elements identified at spot A in Fig. 4 include Cu, Fe, S, Mn and O as the dominant elements due to the prominent peaks of these elements. Other elements at the spot were Al, Ca, Mg and Si and K. These results are similar to the XRF results of the WMC Sample. The results thus confirm the heterogeneous nature of the waste manganese carbonate employed in the study in Fig. 5. From Fig. 6, Pb, O, Mn and S gave the prominent peaks of the spectrograph. The high lead content can be due to presence of galena (PbS) in the sample. Other trace elements at spot B were Si, Al, Fe, Ca and Mg which constitute components of some minerals in the XRD results. The spectrograph in Fig. 7, showed Si, O and C as the major elements identified at the point. Mn was the only trace element found which suggests the presence of some level of rhodochrosite at the spot C. The high Si and O suggest the presence of quartz as the likely dominant mineral at the point. The major peaks of elements identified at spot D in Fig.4 are represented in Fig. 8 as Mn, C, and O which strongly suggest the presence of rhodochrosite at the point as the prevalent mineral. There were also elements such as Si, Al, Ca and Mg in low quantities. The elements found confirm the minerals found in the XRD and XRF analyses conducted. The peaks of major elemental concentrations identified in Fig. 9 were Si, Mg, O and Mn at spot E. There were also elements such as Al and Ca in minute quantities. From Fig. 10, Mn, C and O gave the prominent peaks of the spectrograph and high Mn, C and O contents suggest the presence of rhodochrosite at spot F. Other elements measured at the point were Si, Al, Fe, Ca and Mg which compares with the elemental composition by X-ray fluorescence analysis. It was observed in Fig.11that, Al, Si, K, O and V were the major elements at the point G in Fig. 4. The most likely mineral likely to be present at spot G could be vanadium- muscovite and this compares with XRD results obtained on the WMC sample. Mg and Na were the other trace elements identified at the spot.

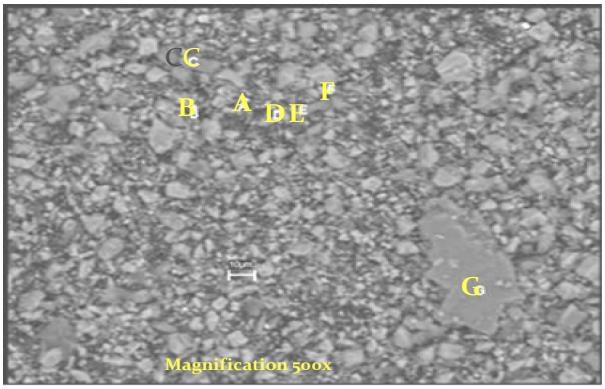

Fig. 4 BSE Image of WMC Sample at Magnification Magnification of 500x at Scale of 10µm

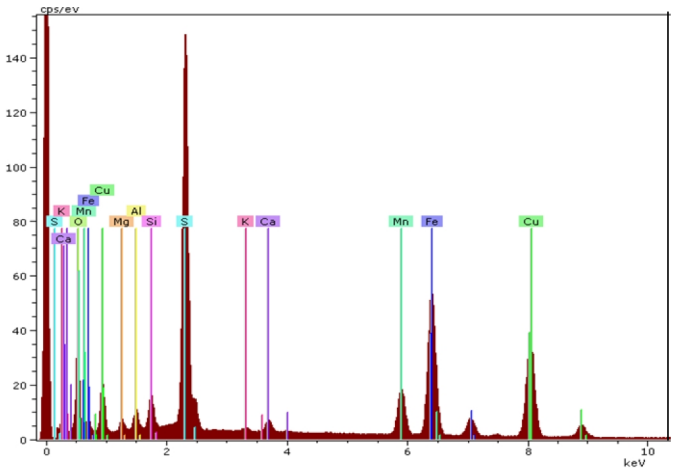

Fig. 5 Spectrograph of Spot A located in Fig. 4

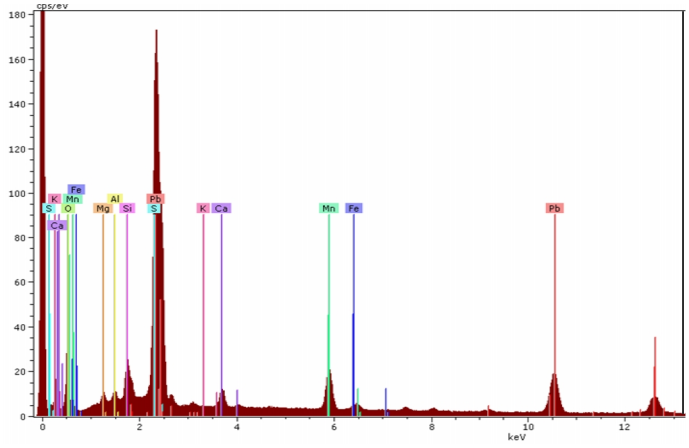

Fig. 6 Spectrograph of Spot B located in Fig. 4

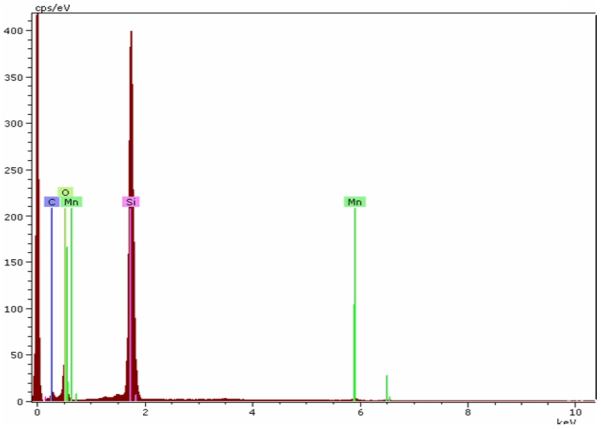

Fig. 7 Spectrograph of Spot C located in Fig. 4

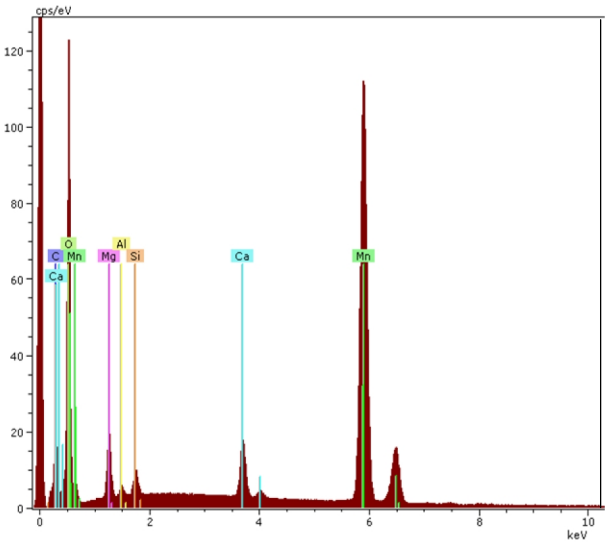

Fig. 8 Spectrograph of Spot D located in Fig. 4

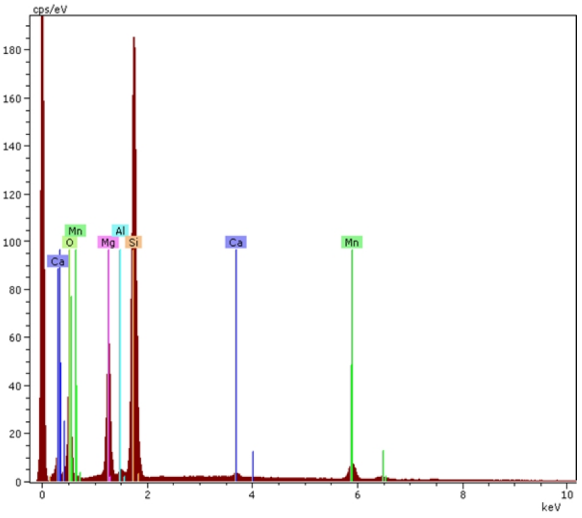

Fig. 9 Spectrograph of Spot E located in Fig. 4

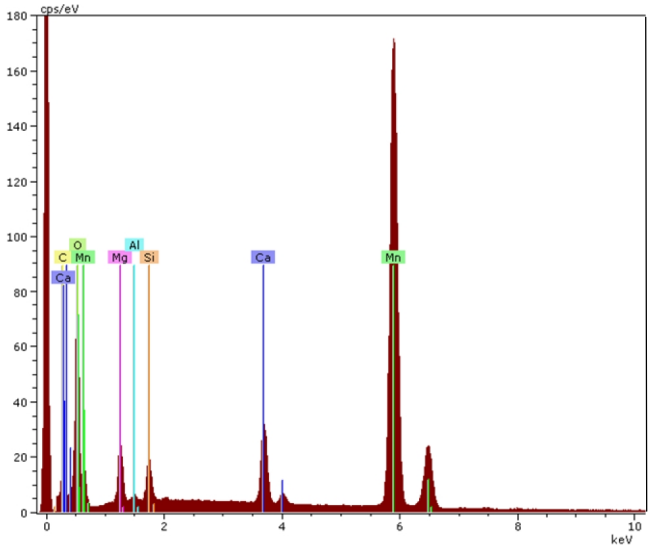

Fig. 10 Spectrograph of Spot F located in Fig. 4

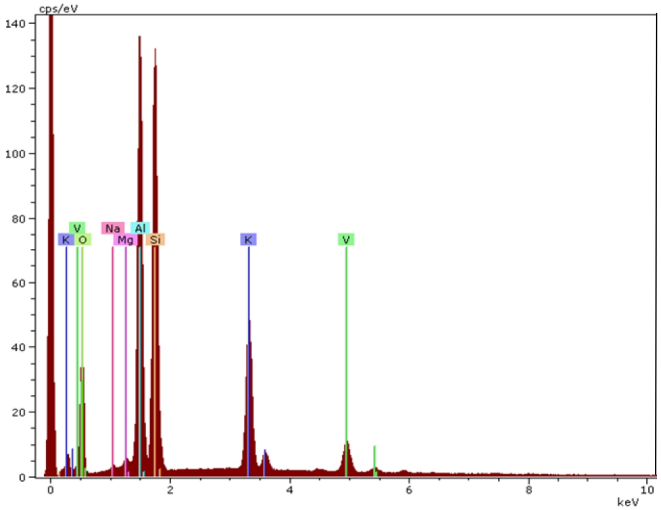

Fig. 11 Spectrograph of Spot G located in Fig. 4

3.5 Analysis and Neutralisation of Biooxidation effluents

Speciation of the biooxxidation effluent was conducted to identify and quantify ions present. The elemental composition is presented in Table 5. The total iron (Fe^{3+} and Fe^{2+}) measured was 4541 mg/L and at pH 1.85 and Eh above 500 mV in the presence of *Acidithiobaccili* species. Magnesium measured in the effluent was 1560 mg/L which may have been solubilised from dolomite present in the flotation concentration biooxidised. Arsenic (As^{5+} and As^{3+}) measured was 1276 mg/L because of biooxidation of arsenopyrite. The sulphate concentration was 8400 mg/L which was primarily H_2SO_4. The high acidity results in low pH of 1.85 can be explained according to the Eh-pH diagram of S-O-H of sulphur system (Brookins, 1987). These can be attributed to pyrite and arsenopyrite minerals treated. The high sulphur solubilisation of

16760 mg/L was due to microbial transformation of sulphur during biooxidation process (Rohwerder and Sand, 2003). Aluminium concentration in the bio-leached effluent was 150 ppm which may exist in ionic forms as Al^{3+} or $AlOH^{2+}$ according to Eh-pH diagram of Al-O-H system (Brookins, 1987). The calcium content measured was 600 mg/L as Ca^{2+} (Brookins, 1987). The presence of phosphorus (3.5 mg/L) may have resulted from addition of phosphoric acid during the biooxidation process as a nutrient requirement of the microorganisms. Silicon measured was 110 mg/L which may have been stabilised in the effluent as H_2SiO_4 as can be shown on Eh-pH diagram of Si-O-H system (Brookins, 1987). The Total Organic Carbon (TOC) measured in the effluent was 21 mg/L which can be due to the presence of organic matter of the material treated and biomass of the microorganisms (Rawlings *et al*., 2003). Trace elements measured in the effluent were vanadium and chromium and many others as shown in Table 6. It can be inferred that, the high levels of ions particularly arsenic in the effluent will pollute the environment; hence the effluent must be treated to remove the toxic ions.

Table 5 Major Components of Bio-Leached Effluent

Elements	Concentration (mg/L)	Elements	Concentration (mg/L)
Al	150	Mn	200
As	1276	S	16760
Ca	600	Si	110
Fe	4541	Mg	1560

Table 6 Trace Elements measured in Bio-Leached Effluent

Elements	Concentration (mg/L)	Elements	Concentration (mg/L)
V	24	Cd	3.4
Cr	54	Sn	0.9
Co	1.3	Cs	6.5
Ti	0.09	Ba	8.9
Ni	2.9	La	13
Cu	2.0	Ce	18
P	3.5	Hf	1.6
Zn	1.7	Ta	1.6
Ga	0.6	Pb	1.1
Rb	0.2	Bi	0.7
Y	1.7	Th	0.7
Zr	0.5	U	2.2
Nb	1.3		

3.6.1 Effect of WMC Particles Concentration on pH of Biooxidation Effluent

The WMC sample neutralisation reactions were slowly exothermic and the exothermic reactions increased moderately with increase in solid concentration. The WMC particles reacted pretty slowly resulting in gentle rise of pH occurring from 1.85 to about 5.0 within 120 min as solid concentrations increased (Fig. 12). There was therefore steady rise in pH with increased solid loading which is due to increased particles as solids increased which increased reacting surfaces for reaction hence deprotonation is increased. However, deprotonation tends to decrease with increased particle loading. This can be attributed to the fact that, as solid loading increased, the reaction rate increased and carbon dioxide formation in solution increased but as the reaction is slowly exothermic, carbon dioxide in solution increase and the gas tends to react with water to produce carbonic acid which thereby tends to protonate the reaction system. Hence the increase in pH with increased solid loading is slowed down as solid concentration increased (Tsunekawa and Takamori,1987). Hence, use of WMC is suitable to achieve precipitation of $FeAsO_4$ between pH ranges of 3.5 and 5.5. However, environmental pH would be difficult to attain despite high solids concentrations. Hence lime will be required to increase pH during effluent neutralisation to attain environmental conditions.

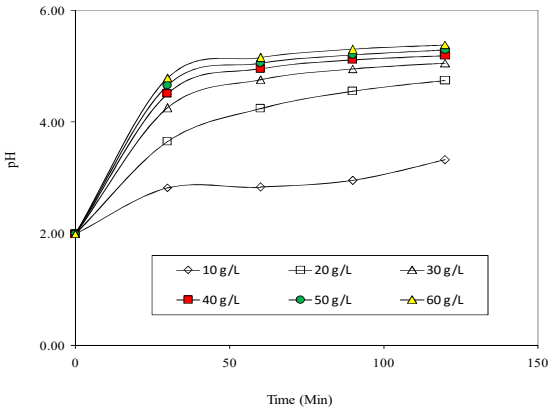

Fig. 12 Effect of WMC Particle Concentration on pH of Biooxidation Effluent Neutralisation

3.6.2 Effect of WMC Particle Concentration on arsenic sequestration from Biooxidation Effluent

The results showed that WMC particle concentration increased sequestration of arsenic in solution as is presented in Table 7. It was observed that, 10 g/L WMC concentration, reduced arsenic from 1276 mg/L to 1.11 mg/L after 360 min of stirring and at 60 g/L WMC concentration, arsenic in solution decreased to 0.78 mg/L which can be attributed to increase in particle concentration in the solution.

Table 7 Arsenic in Solution against Varying WMC Concentration

WMC (g/L)	10	20	30	40	50	60
As in Soln (ppm)	1.11	1.06	1.00	0.89	0.80	0.78

3.7 Stability of WMC Precipitates

The stability of precipitates formed from treatment of biooxidation effluent with waste manganese carbonate (WMC) material was investigated using Toxicity Characteristic Leaching Procedure (TCLP). The results in Table 8 showed that, precipitates leached at pH 7.0 released 4.135 mg/L arsenic into solution from 40 g/L precipitate. However, when the leach process was carried out at the same solid concentration at pH 7.40, mobile arsenic concentration in solution reduced significantly to 1.594 mg/L. Both of these values are below the maximum allowable threshold of 5 mg/L. Further observation of the process revealed that, increasing solid concentration of the WMC during biooxidation effluent neutralisation, led to a decrease in mobile arsenic concentration making the precipitates generated more stable for dumping. This means that, the particle surfaces are able to hold arsenic more tenaciously.

Table 8 Mobile Arsenic from WMC Precipitate Leach against EPA Value

Sample ID	40 g/L pH 7	50 g/L pH 7	60 g/L pH 7	40 g/L pH 7.4	60 g/L pH 7.4
Mobile As (mg/L)	4.135	3.018	0.899	1.594	0.709
EPA Value	5	5	5	5	5

3.8 Analysis of Precipitates formed at pH 4.5

Backscattered scanned electromicroscopy (BSE) conducted at 900x magnification on the WMC precipitate at pH 4.5 is shown in Fig. 13. The morphology of the particles showed that, the particles were independent and mostly irregular in shape. The particles were finely dispersed and interspersed with medium and relatively large grains. This is an indication that, new minerals precipitated from solution. The surfaces of the particles showed roughness which looked like overgrowth on the surfaces and most fine particles turn to cluster. The precipitates also have sharp edges of the particles. Some of the particles also have grooves on the surfaces which further proves the presence of precipitates formed. The particles also existed in clusters. There are scattered dark spots which suggests the presence of non metallic compounds. Thus, EDS analysis of the spot gave the spectrograph in Fig. 14. The elements therefore measured from the circle of Fig. 13 showed that O, Ca, Mn, S, Al, Fe, Si, Na, Mg, As, P and K were the resolved elements. Thus, from Table 9, the absence of carbon implies absence of a carbonate and the high manganese content might have formed a new compound which did not resolve in the minerallogical results reported by the XRD of the precipitates. From the EDS analysis, the amount of iron precipitated was 2.63% and 0.96 % of arsenic seuestered. This suggests that WMC material can precipitate multi stable compounds from biooxidation effluent.

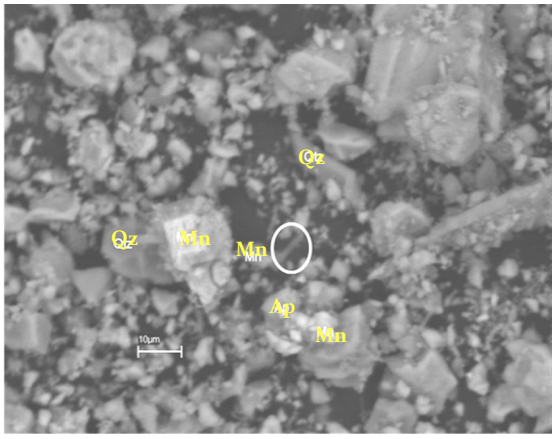

Fig. 13 BSE Image of WMC Precipitate at pH 4.5 at 900x Magnification

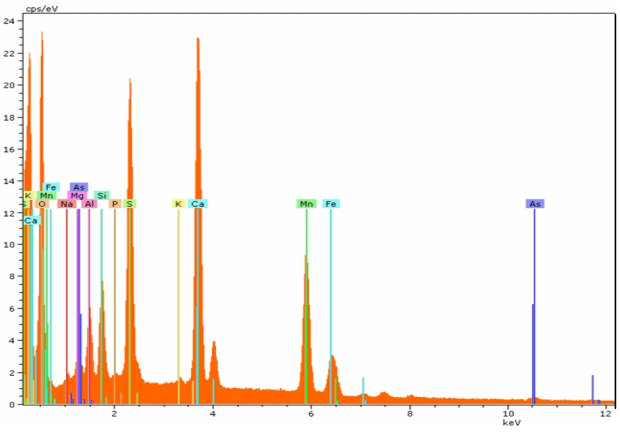

Fig. 14 Spectrograph of Circle in Fig. 13

Table 9 EDS Results of WMC Precipitates

Elements	Wt%	Elements	Wt%
O	54.37	S	9.10
Na	1.70	K	0.23
Mg	1.09	Ca	14.49
Al	2.91	Mn	9.73
Si	2.54	Fe	2.63
P	0.24	As	0.96

3.9 Analysis of WMC Precipitates formed at pH 7

SEM investigation of WMC precipitate at pH 7 at 1000x magnification is shown in Fig. 15. It was observed that, the particles were predominantly very fine with a few medium and large sizes which were irregularly shaped and mostly clustered. Some of the particles were needle-like as indicated by the arrow; others were cylindrical in shapes which were mostly with smooth surfaces. The larger particles had rough surfaces as with small precipitates over their surfaces. Most of the particles were also clustered and there were voids in between the clusters. The arrow shows the particle from which the EDX spectrum was collected. According to the EDS results of the spot shown by arrow in Fig. 15, the spectrographic analysis in Fig. 16 showed that, Fe, Mn, As, Ca, S, Si, C and O were the major elements. The elemental concentration is shown in Table 10 and the percentage content is found to range from 0.72% for K to 53.68% for oxygen at the point.

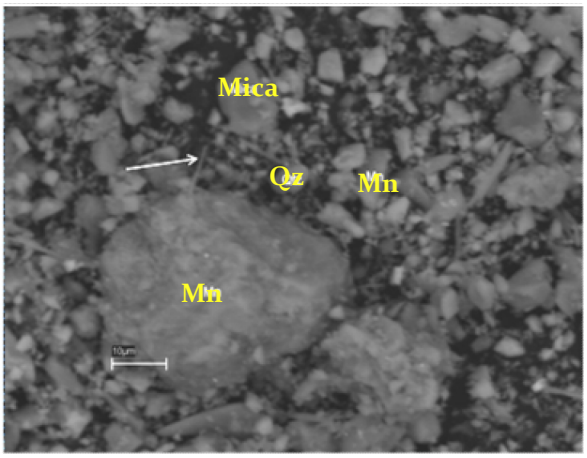

Fig. 15 BSE image of WMC Precipitate at pH 7

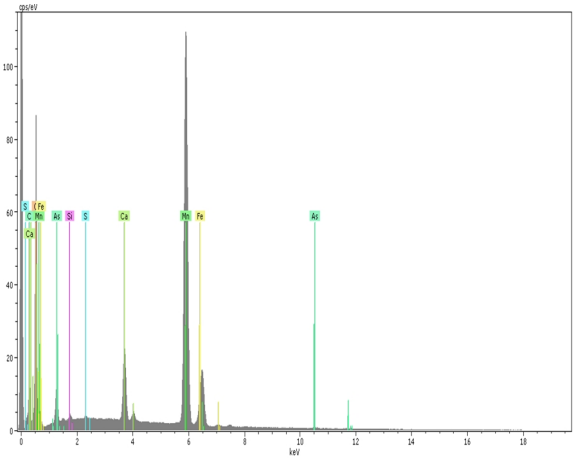

Fig. 16 Spectrograph at Arrowed Point of pH 7 of WMC Precipitate in Fig. 15

Table 10 EDS Results of WMC Precipitate in Fig. 15

Spectrum	Wt%	Spectrum	Wt%
O	53.68	Si	5.86
Na	0.82	K	0.72
Mg	1.32	Ca	10.77
Al	2.73	Mn	16.95
Si	2.60	Fe	3.42
		As	1.12

3.10 Specific Surface Area of WMC Precipitates

The specific surface area measured for WMC neutralised precipitate was 12.62 m^2/g after neutralisation at pH 7.0 indicates the slower chemical reaction exhibited by the WMC sample (Allen 1997, 1992,). Furthermore, adsorption cumulative volume pore sizes between 1.70 and 300 nm reduced from 0.012 cm^3/g to 0.009 cm^3/g at pH 7 which suggests that precipitation occurred in the pores. WMC precipitates contain larger particles and as such settleability in tailings impoundment can be enhanced and sliming reduced.

3.11 Particle Size Distribution of Reacting WMC Particles

The particle size distribution of reacting particles at neutralisation pH of 4.5 showed that, the D_{50} increased from 5.890 to 10.35 µm which can be attributed to precipitation/adsorption of WMC. However, particle size distribution at pH 7.0 showed that the D_{50} of the WMC material decreased to 10.17 µm which can be due to continuous dissolution of manganese.

4 Conclusions

It can be concluded that, milling Waste Manganese Carbonate (WMC) has medium grindability with Bond index of 13.52 kWh/t. The mineralogical compositions of Waste Manganese Carbonate are manganese carbonate (76.6%), dolomite (7.1%), muscovite (8.5%), quartz (6.5%), todorokite (0.3%) and the amorphous content was 1.0%. Chemically, the WMC material contains approximately 28.26% elemental Mn. The isoelectric point of WMC particles in milliQ water was at ~pH 8.5. Initial surface area of WMC powder was 6.12 m^2/g but the precipitate surface area was 12.62 m^2/g after neutralisation at pH 7.0. In a similar manner, the D_{50} of WMC sample increased from 5.89 µm to 10.35 µm for the precipitate formed at pH 4.5.The WMC powder is able to deprotonate biooxidation effluent from pH 1.85 to 5.5 in 120 min depending

on solid loading. Beyond this value, increase in pH could be achieved with minimal addition of lime. Arsenic sequestration increased with increasing WMC concentration. Mobile arsenic extracted from the precipitate averaged 4.135 mg/L at pH 7.0 and 1.594mg/L at pH 7.4 as against the EPA maximum allowable concentration of 5.0 mg/L.

Acknowledgements

The author is grateful to the Government of Ghana through The GETfund and Management of The University of Mines and Technology for the financial support for this project. The author is also grateful to The Ian Wark Institute of the University of South Australia (UNiSA) for the opportunity to carry out Laboratory experiments and analyses of samples at the Institute. The author is also very grateful to the management of Sulphide Treatment Plant (STP) of AngloGold Ashanti Limited Obuasi Mine for permission to use their facility to perform major laboratory tests at the Metallurgical and Chemical Laboratories.

References

Allen, T. (1992), "Particle Size Measurement", *Journal of Dispersion Science and Technology*, Volume 13, Issue 5. pp. 1-8.

Allen, T. (1997),*Particle Size Measurement, Volume 1, Powder sampling and particle size measurement methods*, Chapmann & Hall, London. pp. 1-53.

Anon (2015), "Surface Area by Gas Sorption", Quantachrome Instruments, *www.quantachrome.com*Accessed on 12.06.15.

Anon (2017), The mineral rhodochrosite *www.minerals.net/mineral/rhodochrosite.aspx***.** Accessed on 01.03.17.

Bennet, J. C. and Tributch; H. (1978), "Bacterial leaching patterns on pyrite crystal surfaces", *J.Bacteriol,* 134, pp. 310-317.

Brookins, D. G. (1987), *Eh-pH Diagrams for Geochemistry*. Springer-Verlag, Berlin Heidelberg, New York. pp. 95 – 96.

Brookins, D. G. (1987), *Eh-pH Diagrams for Geochemistry*. Springer-Verlag, Berlin Heidelberg, New York. p. 165.

Brunauer, S., Emmett, P. H. and Teller, E. (1938),"Adsorption of gases in multimolecular layers". *Journal of the American Chemical Society*, 60, pp. 309–319.

Calvert, S. E. and Price, N. B. (1972), "Diffusion and reaction profiles of dissolved manganese in the pore waters of marine sediments". *Each and Planetary Science Letters*, 16, pp. 245-249.

Duckworth, O. W. and Martin, S. T. (2004), "Role of molecular oxygen in the dissolution of siderite and rhodochrosite". *Geochimica et CosmochimicaActa*, 68, pp. 607–621.

Du Plessis, P. and Maree, J. P., (1994), "Neutralization of acid water in the chemical industry with limestone." *Wat. Sci. Tech*., 29 (8), pp. 93-104.

Gahan, C. S.; Sundkvist1, J-E.; Engström, F. and Sandström, Å. (2010), "Comparative assessment of industrial oxidic by-products as neutralising agents in biooxidation and their influence on gold recovery in subsequent cyanidation". Proceedings of the XI International Seminar on Mineral Processing Technology (MPT-2010). Editors: R. Singh, A. Das, P. K. Banerjee, K. K. Bhattacharyya and N. G. Goswami, pp. 1293-1302.

Hamester, M. R. R.; Balzer, P. S.; Becker, D. (2012), "Characterization of calcium carbonate obtained from oyster and mussel shells and incorporation in polypropylene". *Materials Research*; 15(2), pp. 204-208.

Isa, A. H.; Abdulrahman, F. W.; Aliyu, H. D. (2014), "BET Surface Area Determination of Calcium Oxide from Adamawa Chalk Mineral Using Water Adsorption Method, for Use as Catalyst". *Chemistry and Materials Research,* Vol.6 No.1, pp. 87-92.

Jensen, D. L; Boddum, J. K.; Tjel, J. C. and Christensen, T. H. (2002), "The solubility of rhodochrosite ($MnCO_3$) and siderite ($FeCO_3$) in anaerobic aquatic environments." *Applied Geochemistry*, 17, pp. 503-511.

Johnson, S. B., Franks, G. V., Scales, P. J., Boger, D. V. and Healy, T. W. (2000), "Surface Chemistry-Rheology Relationships in Concentrated Mineral Suspensions",*International Journal of Mineral Processing*, 58, pp. 267-304.

Kesse, G. O. (1985), *The mineral and rock resources of Ghana*, A. A. Balkema/Rotterdam/Boston. pp. 298-338, 582.

Lindström, E. B.; Gunneriusson, E. and Tuovinen, O. H. (1992), "Bacterial oxidation of refractory ores for gold recovery". *Crit Rev Biotechnol*; 12, pp.133–55.

Maree, J. P. and Du Plessis, P. (1994), "Neutralization of acid mine water with calcium carbonate." *Wat. Sci. Tech.* 29 (9), pp. 285-296.

Marshall, K. C. M., Pembrey, R., Schneider, R. P. (1994), "The relevance of X-ray photoelectron spectroscopy for analysis of microbial cell surfaces: a critical review". *Colloids Surf B Biointerfaces*, 2, pp. 371–376.

Napier-Munn, T. J., (1996), *Mineral Comminution Circuits: Their Operation and Optimisation,* Julius Kruttschnitt Mineral Research Centre, Isles Road, Indooroopilly, Queensland 4068, Australia, 413 pp.

Olivier, J. W., Van Niekerk, J. A., Chetty, K. R. and Ahern, N. (2000). "Biox plant nutrient

optimisation." In: Proceedings of the *Colloquim Bacterial Oxidation for the recovery of metal Johannesberg*, pp. 1-6.

Olivier, W. (2001), "Flotation Tailings as neutralizing agent: Bogosu pilot run." In: Proceeding of the *4th Biox users group meeting, Wiluna*, pp. 30-38.

Pantuzzo, F. L. and Ciminelli, V. S. T. (2010),"Arsenic association and stability in long-term disposed arsenic residues". *Water research*, 44, pp. 5631- 5640.

Rohwerder, T., Sand, W. (2003), "The sulfane sulfur of persulfides is the actual substrate of the sulfur-oxidizing enzymes from Acidithiobacillus and Acidiphilium spp." *Microbiology*, 149, pp. 1699–1709.

Starkey, J. H. and Meadows, D. (2007), Comparison of Ore Hardness Measurements for Grinding Mill Design for the Tenke Project. *CMP Conference Proceedings,* pp. 19-31.

Swash, P. M. and Monhemius, A. J. (2014), "Aspects of arsenical materials and their long term stability under environment conditions", *MIRO Arsenic Research Group*, Imperial College of Science Technology and Medicine, London, SW7 2BP. pp. 1 - 15.

Swash, P. M. and Monhemius, A. J. (1994), "Hydrothermal precipitation from Aqueous solution containing iron (III), arsenate and sulphate." (*Hydrometallurgy'94* New York: Chapman and Hall), pp. 177-190.

Ticknor , K. V. and Saluja, P. P. S (1990), "Determination of Surface Areas of Mineral Powders by Adsorption Calorimetry" *Clays and Clay Minerals*, Vol. 38, No. 4, pp. 437-441.

Tsunekawa, M. and Takamori, T. (1987), "An aspect of interfacial characteristics of carbonate minerals in water". *Department of Mineral Resources development Engineering*, Faculty of Engineering, University of Hokaido University, Sapporo, 060, Japan. pp. 132-144.

Wersin, P.; Charlet, L.; Karthein, R. and Stumm, W. (1989), "From adsorption to precipitation: Sorption of Mn^{2+} on $FeCO_3$." *Geochimica et Cosmochica Acta*, 53, pp. 2787-2796.

Zhu, Y. N., Zhang, X. H., Xie, Q. L., Wang, D. Q., and Cheng, G. W. (2006), "Solubility and stability of calcium arsenates at 25 °C". *Water, Air and Soil Pollution*, 169, pp. 221–238.

Authors

Joseph J. K. Gordon is a Lecturer at the University of Mines and Technology (UMaT) Tarkwa. He holds MPhil and BSc degrees in Metallurgical Engineering from Kwame Nkrumah University of Science and Technology (KNUST) Kumasi. His research activities are in Biohydrometallurgy, Mine Waste Processing and characterisation. He is a member of the American Society for Quality (ASQ).

E. K. Asiam is an Associate Professor of Minerals Engineering. He holds a BSc and PhD degrees from the Kwame Nkrumah University of Science and Technology (KNUST), Kumasi. He lectures in Heap Leaching Technology, Alluvial Mining, Hydrometallurgical Applications, Metallurgical Plant Design and Operations and Environmental Management and Safety. He has researched and consulted extensively on processing of refractory gold ores and environmental quality assessment and management.